ORIGINAL ARTICLE

Qualified sperm selection based on the rheotaxis and thigmotaxis in a microfluidic system

Nima Ahmadkhani[1] · Maryam Saadatmand[1] · Somaieh Kazemnejad[2] · MohammadJafar Abdekhodaie[1]

Abstract

Microfluidic systems with the ability to mimic the female reproductive tract (FRT) and sperm features have emerged as promising methods to separate sperm with higher quality for the assistant reproductive technology. Thereby, we designed and fabricated a microfluidic system based on FRT features with a focus on rheotaxis and thigmotaxis for passive sperm separation. In this regard, four various geometries (linear, square, zigzag, and sinusoidal) were designed, and the effect of rheotaxis and thigmotaxis were investigated. Although separated sperm in all microchannels were 100% motile, non-linear geometries were more effective than linear geometry in the term of separating the progressive sperm with high quality. In the presence of upstream flow, periodical changes in the slope of walls (in non-linear geometries) give rise to the periodical facing sperm with a high flow rate in the middle of microchannels, which was a reason for the high quality of separated sperm. However, because of sharp corners in the square and zigzag microchannels that create dead zones with a lack of upstream flow, which is noticeable via simulation results, these geometries have obstacles against sperm swimming toward the outlet, which was proved by image analysis. The sinusoidal geometry showed the highest enhancement level of the designed geometries compared to the linear geometry. Separated sperm exhibited 34.7% normal morphology, 100% motility, and 100% viability in the sinusoidal geometry. Therefore, the periodic change in the position of sperm from one wall to another wall can be a strategy for separating sperm with high quality.

Graphical abstract

In the present study, we used a microfluidic system for studying the combined effects of thigmotaxis and rheotaxis for sperm separation process to achieve the successful Assisted reproductive technology (ART). The designed PDMS-based microfluidic system had four various geometries, including linear, square, zigzag, and sinusoidal. The functionality of separated sperm was evaluated by sperm tracking (ImageJ), motility assay (CASA software), and morphology assay (Papanicolaou ultrafast staining). Probing various geometries revealed 100% motility. In non-linear geometries, sperm's periodic detachment from the walls gave rise to the periodic interaction with the high flow velocity in the center of the channel, resulting in the separation of high-quality sperm with progressive motility. The collected data proved the influence of thigmotaxis on the quality

✉ Maryam Saadatmand
m.saadatmand@sharif.edu

1 Department of Chemical and Petroleum Engineering, Sharif University of Technology, 11155-9465, Tehran, Iran

2 Nanobiotechnology Research Center, Avicenna Research Institute, ACECR, Tehran, Iran

of separated sperm. Morphologically improvement in separated sperm from the sinusoidal geometry was significant than others, which means the sinusoidal structure would be the best candidate for the sperm separation process.
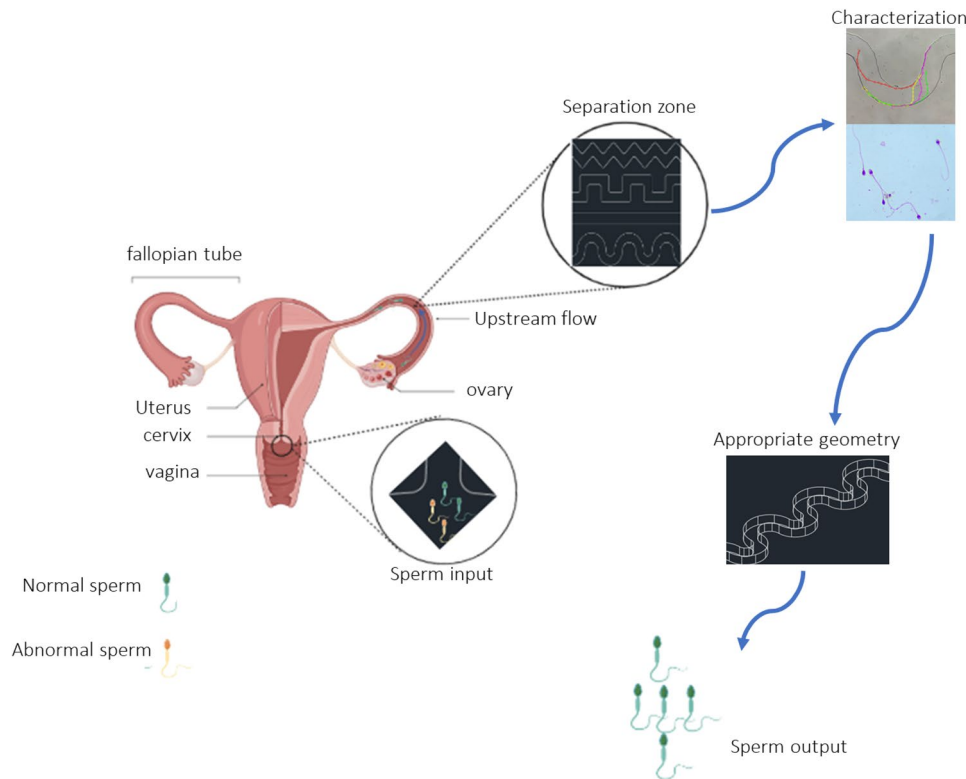
Keywords Microfluidic system · Sperm separation · Rheotaxis · Thigmotaxis · Female reproductive tract

1 Introduction

The rising infertility trend globally highlights the urgent need to improve the assistant reproductive technology (ART) related challenges. Worldwide, more than 50 million couples struggle with infertility [1], 20–70% of which approximately originate from malefactors [2]. For the couples with malefactor infertility issues, intracytoplasmic sperm injection (ICSI) is an ART method used prevalently [3, 4]. It is imperative to choose functional sperm with normal morphology and motility for ICSI to be successful [1, 5]. However, studies have shown that conventional sperm separation methods, density gradient centrifuges (DGCs) and swim-ups, are less effective for sperm selection. Several factors contribute to this, including bypassing the natural process of sperm separation in the female reproductive tract (FRT), damaging sperm DNA by increasing reactive oxygen species (ROS), reducing yields, and requiring a long processing time [6–9]. To address these defects, researchers have been motivated to develop alternate methods, including non-microfluidic (zeta potential [10, 11], annexin V affinity-based separation [12, 13], hyaluronic acid binding [14, 15] and etc.) and

microfluidic systems [16–18]. New non-microfluidic sperm separation methods still face challenges due to causing DNA damage, low yields, human errors, high costs, and bypassing natural barriers despite their promising results [19].

Microfluidic systems have unique features that make them ideal for separating sperm. Microfluidic systems are able to separate intact normal sperm for patients with a low count of sperm, which is less likely by conventional methods [20, 21]. They separate immotile sperm from microdissection testicular sperm extraction and blood based on sample components size[18, 22, 23]. Additional advantages of these systems are small scale, low amount of waste and required sample, and precise control over the system [7, 24, 25].

In addition, another important feature of microfluidic systems is being able to mimic elements of the natural process of sperm separation. Briefly, in the FRT, sperm faces numerous obstacles and features during its journey toward the oocyte. For instance: fluid properties of different parts of FRT, inclusive of viscous and viscoelastic [26], presence of a thermal difference between beginning and end of the fallopian tube [27, 28], secretion chemoattractant for sperm guidance toward the oocyte [29], structural features of FRT such

as diffuser type in two sides of the cervix and microgrooves on the surface [30, 31], and creation upstream flow by cilia beating and muscle contraction and expansion of FRT [32]. Consequently, researchers are trying to enhance the quality of separated sperm for ART by replicating those barriers individually or in combination [1, 8, 33]. In recent years, high throughput techniques, such as omics approaches, have been widely used to identify and quantify the biological molecules contributing to the cell's structure and function [34, 35]. These studies have also been used to comprehensively understand the biological factors affecting sperm quality [36].

As upstream flow is the dominant feature all over the FRT, giving rise to sperm's rheotaxis behaviour [37–39], recently, some microfluidic systems have been designed to work based on the this feature of sperm [40–43]. The range of velocity to emerge rheotaxis feature of sperm is confined between 22 to 102 μm/s [30, 32]. In order to study sperm rheotaxis behaviour, different structures (microgrooves, diffuser channel, coral system) [30, 44–47], various fluid properties (pH, hyperactivated spermatozoa, viscous and viscoelastic) [26, 48, 49], and sperm flagellar beating patterns [50] have been investigated by microfluidic systems. The results of mentioned studies suggested that rheotaxis response of sperm is an effective factor in sperm behaviour and can be a promising method for sperm separation. A study by Martin et al. showed that separated sperm based on rheotaxis exhibited better morphology and chromatin maturity [51]. Another study developed microfluidic devices using the oval-shaped microstructures of the female fallopian tube to form micropocket geometries. According to their results, separated sperm are highly viable and motile (100% efficiency) [52]. In another study, Nagata et al. used hydrostatic pressure to produce upstream flow; as a result, they separated normal bovine sperm, including acrosome-intact and high mitochondrial activity that consequently increased fertility rate [53]. Sharma et al. showed that separated sperm based on the rheotaxis response of sperm exhibited almost 100% motility, a higher normal morphology, and less DNA fragmentation compared to raw and separated sperm in the device without flow [54].

Thigmotaxis, known as sperm response to the mechanical stimulus (interaction between sperm and boundary walls), was investigated broadly by microfluidic systems [19, 55]. Denissenko et al. designed various geometries to probe sperm's behaviour. They showed that sperm tend to swim near the boundary walls while in the presence of sharp channels turn, they leave the boundary wall that they were swimming and continue swimming at the opposite side [56]. Another study found that normal sperm could swim 5 to 20 times faster than abnormal sperm in microfluidic systems with micropillars. A further finding on the mentioned device suggested that thigmotaxis significantly affects the quality

of separated sperm (52% normal in morphology and 44% nuclear mature) [16]. In light of the results of the mentioned studies, thigmotaxis plays a vital role in sperm separation.

Despite promising results gaining from microfluidic systems, there are still some areas for progress. Most microfluidic systems have not been used upstream flow for human sperm separation. It was proved that sperm swimming trajectories are circular in the absence of flow due to the asymmetrical flagellar beating, making the fortuitous movement of sperm in different directions. This behaviour causes the loss of some normal sperm and a decrease in the number of separated sperm [1, 45]. However, upstream flow stimulates sperm's orientations against the upstream flow and eliminates sperm accidental movements [45]. It may also be possible to improve microfluidic efficiency by using several features simultaneously instead of one feature at a time.

In this study, we investigated the effect of thigmotaxis along with rheotaxis on selected sperm quality. Based on the studies, microchannel geometry has an important impact on sperm's behaviour [56, 57], while it has been neglected in most of the studies done on sperm selection based on the rheotaxis feature. To this end, four different geometries, including linear, square, zigzag, and sinusoidal, were studied in which upstream fluid flow velocity was set at maximum 50 μm/s. Simulating the injection flow rate with the finite element method (FEM) was used to determine the injection rate. In order to reach a comprehensive conclusion, in addition to image analysis, motility and morphology of the separated sperm were also studied. Our results revealed that using non-linear geometries decreased the possibility of reaching non-progressive sperm to the outlet; also, they did not let sperm with defects in geometries like the big head or the bent neck reach the outlet. However, all proposed geometries significantly improved sperm quality in comparison to raw semen; this augment of quality in the sinusoidal microchannel was more tangible than other ones.

2 Materials and methods

2.1 Materials

All the reagents and chemicals were purchased from Sigma-Aldrich, except otherwise mentioned. Nutrient Mixture F-10 Ham with 2% BSA was used as a buffer.

2.2 Microchip design and fabrication

AutoCAD software was used to depict a microfluidic system with four different architectures (linear, square, zigzag, and sinusoidal) to study the effect of the geometry in the presence of upstream flow on sperm locomotion's behaviour and quality in the outlet (Fig. 1a–b). Based on the distance
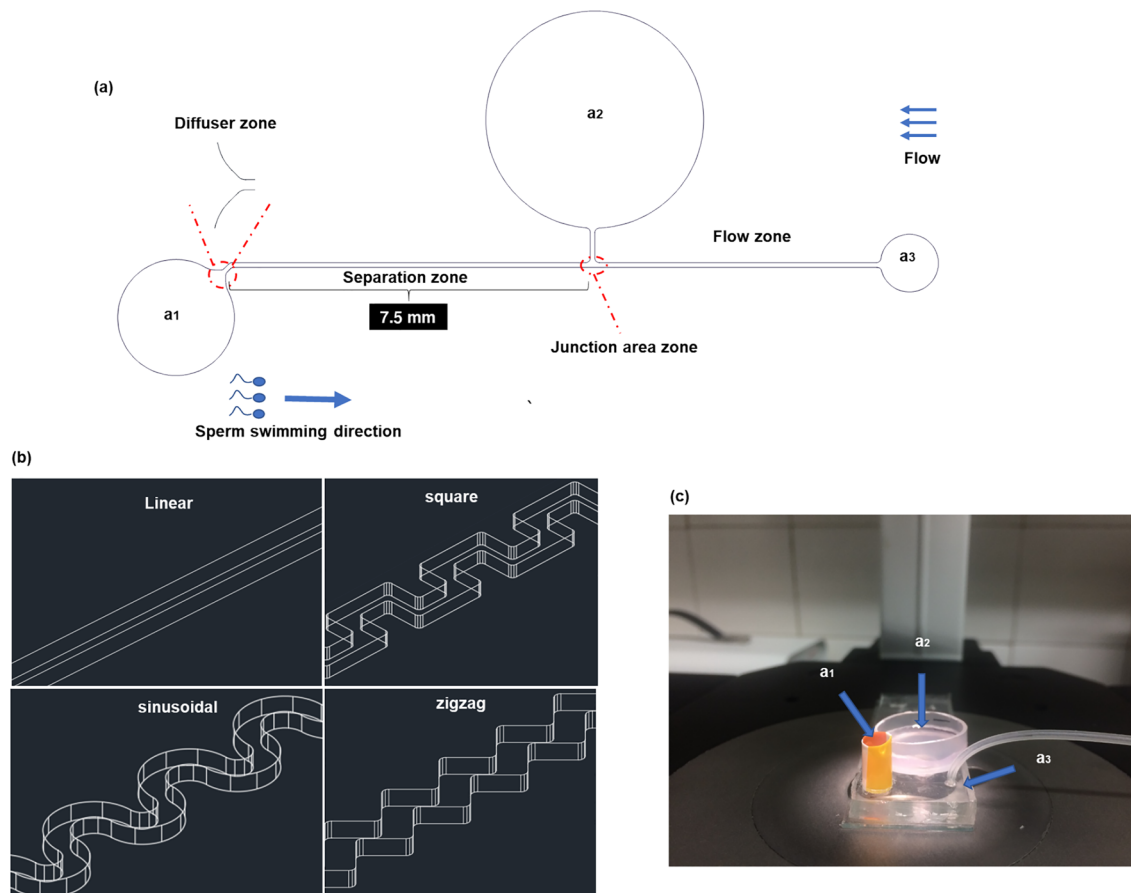
Fig. 1 Schematic and photograph representation of the microfluidic device. **a** The schematic indicates the linear microchannel as a sperm separation device, including reservoir (a$_1$) (diameter of 6 mm) and reservoir (a$_2$) (diameter of 20 mm) and reservoir (a$_3$) (diameter of 1.5 mm). **b** Various geometries of microchannels inclusive of linear, square, sinusoidal, and zigzag. **c** Photograph of a microfluidic device on the microscope stage to do the experiment

among cilia cells and the average length of sperm, 75 and 100 μm were used as height and width of microchannels (100 μm × 75 μm cross-section) [58]. In addition, microchannels (sorting zone) were fabricated with 7.5 mm length (distance between sperm inlet and outlet) [58]. Each structure of microfluidic system was comprised of other parts, including the diffuser type structure, the flow zone, and the junction area (Fig. 1a). Then the silicon mold was fabricated using the standard photolithography method and the SU8 2075 negative photoresist (MicroChem, Newton, MA, USA) by MMT-co. (Tehran, Iran). The PDMS microfluidic device was fabricated using the standard soft lithography method (Fig. 1c). Three reservoirs, including reservoir (a$_1$) (sperm inlet and flow outlet), reservoir (a$_2$) (sperm outlet and flow outlet), and reservoir (a$_3$) (flow inlet), were used in this system. After punching with a biopsy punch, polypropylene cylindrical reservoirs with 6 mm and 20 mm diameters were designed and assembled on the microfluidic system for reservoir (a$_1$) and reservoir (a$_2$), respectively. This was done to prevent flow rate fluctuations in the separation zone

(Fig. 1a). Finally, the PDMS chip was bounded to glass slide by plasma bounding.

2.3 Flow simulation in designed microchips

Four microfluidic systems including linear, square, zigzag, and sinusoidal were modelled using COMSOL MULTIPHYSICS (version 5.2). We used a 2D and stationary laminar fluid module with no-slip boundary conditions at the boundary walls to solve Navier–Stokes (Eq. 1) and conservation of mass (Eq. 2). The simulation was conducted at an inlet flow rate of 0.7 μl s^{-1}.

$$\rho(v \cdot \nabla v) = -\nabla p + \nabla \cdot \mu \left(\nabla v + (\nabla v)^T \right), \tag{1}$$

$$\nabla \cdot v = 0, \tag{2}$$

where v represents the velocity field, ρ is sperm buffer density, p is pressure, and μ is the dynamic viscosity of sperm

buffer. In this experiment ρ and μ were consider equal to water at 37 °C.

2.4 Semen sample preparation

The samples used in this study were waste part of fresh semen samples obtained from healthy men who were referred to the Avicenna fertility center (Tehran, Iran) after taking informed consent. This study was approved by the Institutional Review Board (IRB) of the Biomedical Research Ethics Committee of Academic Center for Education, Culture and Research (ACECR, Tehran, Iran) (ID Number: IR.ACECR.AVICENNA.REC.1398.028). The semen samples were kept in an incubator at 37 °C before injection.

2.5 Experimental procedure

Before starting experiments, all the microchannels and reservoirs were filled with the buffer then vacuum pressure (200 mbar) was applied for about 30 min to remove all the air bubbles from the microchannels. In the next step, all the microchannels and reservoirs (reservoir(a_1) = 180 μl and reservoir(a_2) = 630 μl) were re-filled with the buffer (37 °C) to create enough hydrostatic pressure, which can make the maximum flow rate of ~ 50 μm/s in the separation zone during the separation process. The flow rate of $0.7 \mu l\,s^{-1}$ was conducted to the reservoir (a_3) by the syringe pump (SP1000HSM, Fnm co., Iran) to create a steady condition into the microdevice, then 20 μl of raw semen from a test tube containing 20 million to 40 million sperm per millilitre of semen was injected into the reservoir(a_1). The movement of sperm from the inlet toward the outlet was monitored using Labomed™ TCM 400 Inverted Research Microscope, and the captured movies were evaluated by ImageJ software to track the sperm. 100 μl buffer containing separated sperm was collected from the reservoir(a_2) after 10 min by pipet for conducting assays. Finally, sperm morphology, motility, and movement track were investigated by Papanicolaou ultrafast staining kit (ETCCO), computer-assisted semen analysis (CASA) software (ETCCO), and ImageJ software, respectively.

2.6 Sperm viability and mobility assay

CASA software was employed for probing sperm motility. Based on sperm motility, sperm got divided into three subgroups, including immotile, non-progressive, and progressive. More than 200 sperm were analysed at 60 frames per second (fps) per specimen [59]. In addition, based on the direct relation between viability and motility, sperm viability was concluded [8, 60].

2.7 Sperm morphology assay

Separated sperm were collected from the reservoir (a_2) and assessed using Papanicolaou ultrafast staining kit. Collected sperm were smeared on the glass side and, after air-drying, stained by immersing in several buffers. Labomed LX400 Microscope with $100 \times$ magnification was used for taking images [59]. Sperm morphological classifications were determined based on Bartoov et al. report [61].

3 Results and discussions

3.1 Device working, sperm sorting, and simulation

Upstream flow and thigmotaxis are two fundamental features of FRT that play an essential role in guiding sperm toward oocytes [30]. In this regard, we investigated various geometries (linear, square, zigzag, and sinusoidal) in the presence of upstream flow to separate intact, motile, and morphologically normal sperm. Each structure of microfluidic device comprised of four various zones (diffuser zone, separation zone, junction area zone, and flow zone) brought a suitable opportunity to utilize the effect of the thigmotaxis, motility, and rheotaxis features together on a selection of sperm (Fig. 1). In the first stage, the entrance of sperm into the microchannel, a diffuser-type structure was used for increasing the average number of sperm entering the microchannels by widening the area resulting in decreasing flow velocity of upstream flow. The separation zone was designed with various geometries to study the effect of thigmotaxis. The third zone was the junction zone, where separated sperm washed to the outlet. The last zone was the flow zone that provided the upstream flow to the system.

Pump (reservoir (a_3)) and hydrostatic pressure (specific design of reservoirs (a_1) and (a_2)) were used together for diminishing the plausibility of error in the designed device. The presence of reservoirs with different sizes resulting in the net capillary forces imbalance and height differences in buffers of reservoirs (a_1) and (a_2) helped maintain the steady situation's flow rate. Used hydrostatic pressure in two reservoirs made this system more user-friendly by decreasing the number of pumps from three to one.

The rationale behind this design is that flow velocity near the walls is minimal; therefore, sperm swimming in this position encounter less flow velocity. However, sharp curves in the pathing way of sperm give rise to detachment of sperm from one boundary wall and reach the opposite wall, resulting in their encounter with the high upstream velocity in the middle of a microchannel. Given explanations, sharp curves can make obstacles against non-progressive sperm, leading to a significant increase

in separated sperm quality. On average, the microfluidic system mentioned above retrieved approximately 1200 sperm per 10 min.

Furthermore, by utilizing Comsol Multiphysics, we were able to predict the flow rate and buffer volume required in the reservoirs, ultimately eliminating the need for two additional pumps. Therefore, sperm would show a rheotaxis response in the separation zone (Fig. S1). Assuming that the boundary walls were not slippery, momentum and mass conservation equations could be solved, enabling flow velocity to be calculated in a microfluidic system. According to Fig. S2, the flow velocity in the junction zone and area before the junction zone is significantly higher than that in the separation zone, which supports the observed phenomenon of washing the sperm into the outlet. Fig. S1 and S3. show flow velocity expressed in color and measured using cut lines in the separation zone. Based on the results, the maximum flow velocity for the injection rate flow rate of $0.7\,\mu l\,s^{-1}$ was $\sim 50\ \mu m \cdot s^{-1}$, which is in the rheotaxis response zone of sperm ((Buffer volume in reservoirs (a_1) = 180 μl and reservoir(a_2) = 630 μl). Flow velocity near the boundary walls was zero; however, it was maximum in the middle of the channel ($\sim 50\ \mu m \cdot s^{-1}$). For the corners (zigzag and square), the flow velocity is zero, meaning sperm cannot demonstrate rheotaxis, as shown in Fig. S1. As a result, the above explanation supports sperm confusion at corners, discussed later. It is noteworthy that the simulation predictions proved accurate, as we were able to elicit a rheotaxis response from sperm during the experiment by utilizing the calculated flow velocity and required buffer volume in the reservoirs. Furthermore, the simulation data provided an explanation for some observed phenomena, including sperm confusion in the corners due to dead

zones, emphasizing the significance of upstream flow in redirecting sperm towards the outlet.

3.2 Image analysis

Upstream flow rate gives rise to sperm navigation toward the opposite direction of flow, which can help sperm avoid distraction and bewilderment. Add to this; sperm tend to swim near the wall due to their structure. As it is evident in Fig. 2a, in the linear microchannel, sperm preferred to swim along the wall and scarcely were seen in the middle of the microchannel. Since most sperm swim near the wall without detachment, the possibility of sperm interplay with high flow velocity in the center of the microchannel gets low. Thereby, non-progressive sperm have an opportunity to reach the outlet, which can allude to one of the most significant defects of previous studies to utilize a straight microchannel. However, in the three other microchannels, due to the periodic changes in wall slope, sperm keep their way with the previous slope, in which they have to detach from the boundary wall and reach the opposite side (Fig. 2b, c and d). It is obvious that periodic detachments lead to periodic interactions of sperm with high flow velocity in the center of the microchannels. Among these sperm entering the microchannels, only some of them have the ability to swim against the flow and reach the outlet. On the other hand, some of them are wiped out to the inlet after several interplays with the high flow velocity in the center of the microchannels, which can be associated with the fact that intact sperm have more ability to navigation than the abnormal sperm (Movie S1). Therefore, by proceeding from the inlet toward the outlet, the number of sperm decrease significantly.

Movies S2 and S3 indicate that one of the primary defects of square and zigzag microchannels was dead zones
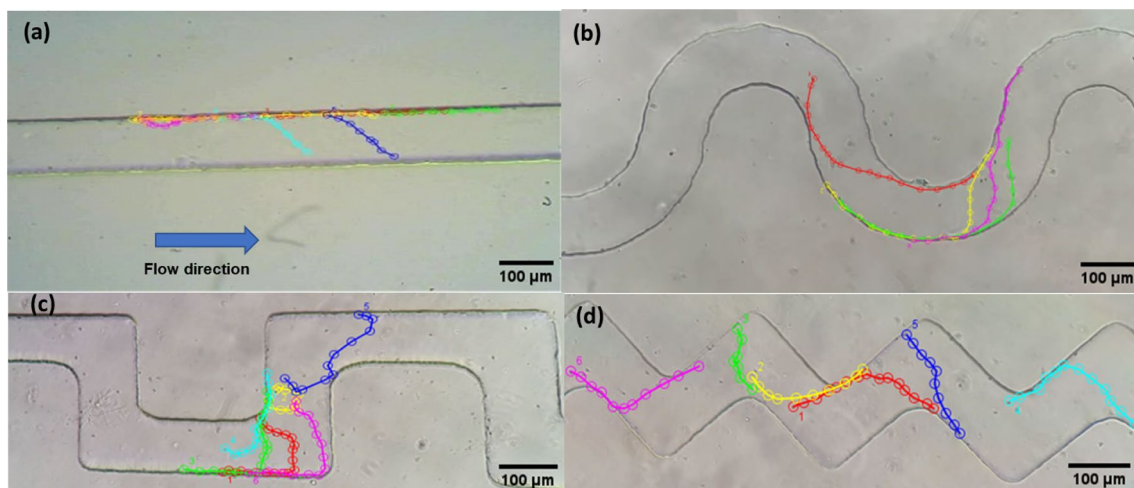

Fig. 2 Human sperm behaviour under the upstream flow. The image analysis of sperm tracking in various geometries. **a** linear. **b** sinusoidal. **c** square. **d** zigzag

in sperm swimming way. Some of the sperm were trapped and assembled into dead zones, making obstruction against sperm movement. Moreover, due to the absence of flow in dead zones, some sperm got confused and started to swim in the same direction of upstream flow until reaching the first change of slop, where they sensed the flow and again began to swim against the flow. Dead zones in the square microchannel were much more than the zigzag microchannel; therefore, the more dead zones, the more effect on sperm congregation and confusion. Due to the absence of dead zones in sinusoidal (Movie S1), this effect was not reported in this geometry.

3.3 Viability and sperm motility assay

Sperm motility plays a pivotal role in sperm quality such that the more progressive sperm in the outlet, the more high-quality sperm are in the outlet. Based on the WHO, sperm motility is one of the important agents in infertility [59]. Moreover, sperm motility can be attested to sperm viability [8, 58]. In this regard, sperm motility before and after the selection was investigated with CASA software. As presented in Fig. 3, separated sperm from different geometries had 100% motility (100% viability). In more detail, significant improvement in sperm motility was proved by almost 43% change (70% in the raw semen to 100% in separated one) in all structures. However, they were distinguished from each other in the quantity of progressive sperm, which were $(80.8 \pm 2.6\%)$, $(90 \pm 3.5\%)$, $(92 \pm 1.9\%)$, and $(92.4 \pm 1.8\%)$

for linear, square, zigzag and sinusoidal microchannels, respectively. It is noteworthy to mention that the quantity of progressive and non-progressive sperm in raw semen were $50 \pm 5\%$ and $20 \pm 4.5\%$, and the rest of it belonged to immotile sperm. Based on the mentioned information, the linear microchannel showed a high percentage of non-progressive sperm in a proportion of other ones $(19.2 \pm 2.6\%)$, while this feature in the best condition was $7.6 \pm 1.8\%$ belonging to the sinusoidal microchannel (Fig. 3). It was reported that the number of progressive sperm directly correlates with the viability of sperm, which means progressive sperm are viable for a longer time compared to non-progressive sperm [58]. As a result, the low percentage of the non-progressive sperm in the non-linear geometries is a sign of thigmotaxis's effect on the quality of sorted sperm, which was in agreement with image analysis results.

3.4 Morphology assay

Sperm morphology is one of the leading agents showing sperm quality. The method of sperm selection after initial separation in ICSI is based on their morphology [16, 62, 63]. In this experiment, raw semen and separated sperm morphologies were studied by Papanicolaou ultrafast staining. As it is obvious in the Fig. 4, there were significant morphologically differences among raw semen and separated sperm (raw: $10.2 \pm 1\%$—linear: $24.3 \pm 2.8\%$—square: $26 \pm 2\%$—zigzag: $31.4 \pm 1.7\%$—sinusoidal: $34.7 \pm 1.5\%$). In spite of the remarkable improvement in sperm morphology, this feature in the sinusoidal microchannel was slightly better than other non-linear geometries. The absence of sperm with a large head and bent neck added great weight to the
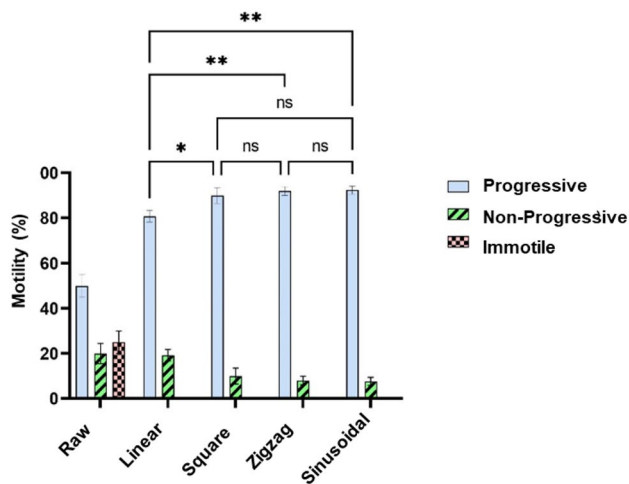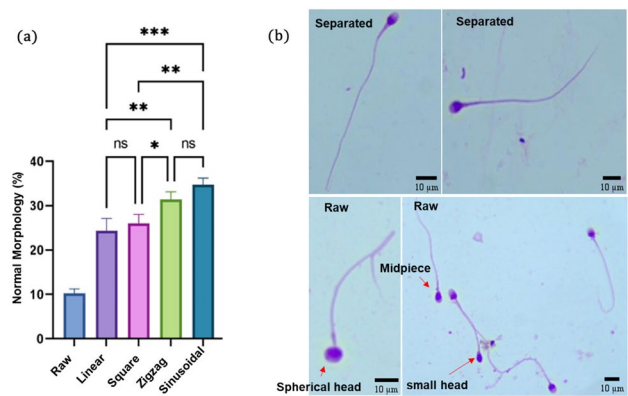
Fig. 3 Sperm motility assay (based on the CASA software) for raw semen and separated sperm with four various geometries. There was no immotile sperm in all geometries, and non-progressive sperm in the sinusoidal geometry was lower than others. Data shown are mean $\pm$ SD for replicates of 3 (n > 200 sperm per replicate). *P*-value was calculated by two-way ANOVA. All of the geometries had a $P < 0.0001$ in comparison to the raw semen. (**$P \leq 0.01$, * $P \leq 0.05$, ns $P > 0.05$)

Fig. 4 Assessment of sperm morphology based on Papanicolaou ultrafast staining kit. a) Morphology analysis of raw semen and separated sperm with four various geometries the result is mean $\pm$ SD for replicates of 3 (n > 100 sperm per replicate). *P*-value was calculated by two-way ANOVA. All of the geometries had a $P < 0.0001$ in comparison to the raw semen. (***$P \leq 0.001$, **$P \leq 0.01$, *$P \leq 0.05$, ns $P > 0.05$). b) Photographs of separated and raw sperm. Arrows show sperm with different defects in raw sample

quality of separated sperm. It is worth mentioning that morphologically improvement in the sinusoidal microchannel ($24 \pm 1.5\%$) was meaningful in comparison to other systems; in more detail, this parameter in multiple channels [64, 65], single-channel [66], and filter-based [67] was 12%, 15%, and 10%, respectively.

4 Conclusions

In this study, we have designed a microfluidic system to investigate the synergic effect of rheotaxis and thigmotaxis on separated sperm quality. This novel microfluidic device is a user-friendly and one-step procedure that separates highly morphologically normal and 100% motile sperm in 10 min. Periodic sperm interactions with the highest upstream velocity in the non-linear microchannels' center, obviously seen by sperm tracing, give rise to sweeping non-progressive sperm toward the sperm inlet. This justifies why various parameters related to healthy sperm, including the number of progressive sperm and morphologically intact sperm in the non-linear microchannels, are much higher than the linear microchannel based on reported results. The sinusoidal geometry has been distinguished from other non-linear microchannels (zigzag and square) by the lack of sperm congregation in the dead zones, proved by image analysis and simulation. Morphologically improvement up to $34.7 \pm 1.5\%$ in the sinusoidal microchannel originates from the mentioned conditions, which is highly significant. Also, any sperm with a bent neck and large head has not been found into the separated sperm by non-linear microchannels. Finally, based on the results, this device is more promising to use instead of conventional methods in the clinic and can be utilized for patients with a low count of normal sperm.

However, microfluidic systems showed promising results in sperm separation, but they are not suitable for high-throughput analysis of sperm. In spite of this limitation, the importance of the limitation may vary depending on how the system will be used. For example, for patients with low sperm counts, microfluidic systems remain a strong candidate for sperm separation. This limitation may also be addressed through the implementation of modifications. For example, increasing the number of microchannels for separation or extending the separation time could increase the number of separated sperm and improve the system's throughput capabilities.

Declarations

References

1. Nosrati R, Graham PJ, Zhang B, Riordon J, Lagunov A, Hannam TG, et al. Microfluidics for sperm analysis and selection. Nat Rev Urol. 2017;14(12):707–30. https://doi.org/10.1038/nrurol.2017.175.

2. Leung ETY, Lee CL, Tian X, Lam KKW, Li RHW, Ng EHY, et al. Simulating nature in sperm selection for assisted reproduction. Nat Rev Urol. 2022;19(1):16–36. https://doi.org/10.1038/s41585-021-00530-9.

3. Esteves SC, Roque M, Bedoschi G, Haahr T, Humaidan P. Intracytoplasmic sperm injection for male infertility and consequences for offspring. Nat Rev Urol. 2018;15(9):535–62. https://doi.org/10.1038/s41585-018-0051-8.

4. Palermo GD, O'Neill CL, Chow S, Cheung S, Parrella A, Pereira N, et al. Intracytoplasmic sperm injection: state of the art in humans. Reproduction. 2017;154(6):F93–110. https://doi.org/10.1530/REP-17-0374.

5. Zhou ZH, Kang YJ, Xu ZG, Xue P. Development and prospects of microfluidic platforms for sperm inspection. Anal Methods. 2019;11(36):4547–60. https://doi.org/10.1039/c9ay01641d.

6. Matsuura K, Takenami M, Kuroda Y, Hyakutake T, Yanase S, Naruse K. Screening of sperm velocity by fluid mechanical characteristics of a cyclo-olefin polymer microfluidic sperm-sorting device. Reprod Biomed Online. 2012;24(1):109–15. https://doi.org/10.1016/j.rbmo.2011.09.005.

7. Kashaninejad N, Shiddiky MJA, Nguyen NT. Advances in microfluidics-based assisted reproductive technology: from sperm sorter to reproductive system-on-a-chip. Adv Biosyst. 2018;2(3):1700197. https://doi.org/10.1002/adbi.201700197.

8. Samuel R, Feng HD, Jafek A, Despain D, Jenkins T, Gale B. Microfluidic-based sperm sorting & analysis for treatment of male infertility. Transl Androl Urol. 2018;7(Suppl 3):S336–47. https://doi.org/10.21037/tau.2018.05.08.

9. Suarez S, Wu M. Microfluidic devices for the study of sperm migration. MHR: Basic Sci Reprod Med. 2016;23(4):227–34. https://doi.org/10.1093/molehr/gaw039.

10. Duarte C, Nunez V, Wong Y, Vivar C, Benites E, Rodriguez U, et al. Impact of the Z potential technique on reducing the sperm

DNA fragmentation index, fertilization rate and embryo development. JBRA Assist Reprod. 2017;21(4):351–5. https://doi.org/10.5935/1518-0557.20170055.

11. Khajavi N, Razavi S, Mardani M, Tavalaei M, Deymeh M, Nasresfahani MH. Can Zeta sperm selection method, recover sperm with higher DNA integrity compare to density gradient centrifugation? IJRM. 2009;7(2):73–8.

12. Paasch U, Grunewald S, Glander HJ. Sperm selection in assisted reproductive techniques. Soc Reprod Fertil Suppl. 2007;65:515–25.

13. Gil M, Sar-Shalom V, Melendez Sivira Y, Carreras R, Checa MA. Sperm selection using magnetic activated cell sorting (MACS) in assisted reproduction: a systematic review and meta-analysis. J Assist Reprod Genet. 2013;30(4):479–85. https://doi.org/10.1007/s10815-013-9962-8.

14. Kim SJ, Kim H, Kim TH, Jeong J, Lee WS, Lyu SW. Effect of sperm selection using hyaluronan on fertilization and quality of cleavage-stage embryos in intracytoplasmic sperm injection (ICSI) cycles of couples with severe teratozoospermia. Gynecol Endocrinol. 2020;36(5):456–9. https://doi.org/10.1080/09513590.2019.1681960.

15. Witt KD, Beresford L, Bhattacharya S, Brian K, Coomarasamy A, Cutting R, et al. Hyaluronic acid binding sperm selection for assisted reproduction treatment (HABSelect): study protocol for a multicentre randomised controlled trial. BMJ Open. 2016;6(10):e012609. https://doi.org/10.1136/bmjopen-2016-012609.

16. Chinnasamy T, Kingsley JL, Inci F, Turek PJ, Rosen MP, Behr B, et al. Guidance and self-sorting of active swimmers: 3D periodic arrays increase persistence length of human sperm selecting for the fittest. Adv Sci (Weinh). 2018;5(2):1700531. https://doi.org/10.1002/advs.201700531.

17. Fernandes BD, Dos Santos FA, Bezerra LGP, de Brito PD, de Macedo LB, da Silva AR, et al. Development of a microfluidic system structured on a modified polydimethylsiloxane device for the selection of bovine epididymal spermatozoa. Reprod Toxicol. 2022;110:1–8. https://doi.org/10.1016/j.reprotox.2022.03.005.

18. Jeon H, Cremers C, Le D, Abell J, Han J. Multi-dimensional-double-spiral (MDDS) inertial microfluidic platform for sperm isolation directly from the raw semen sample. Sci Rep. 2022;12(1):4212. https://doi.org/10.1038/s41598-022-08042-1.

19. Ahmadkhani N, Hosseini M, Saadatmand M, Abbaspourrad A. The influence of the female reproductive tract and sperm features on the design of microfluidic sperm-sorting devices. J Assist Reprod Genet. 2022;39(1):19–36. https://doi.org/10.1007/s10815-021-02377-w.

20. Knowlton SM, Sadasivam M, Tasoglu S. Microfluidics for sperm research. Trends Biotechnol. 2015;33(4):221–9. https://doi.org/10.1016/j.tibtech.2015.01.005.

21. Panah AG, Targhi MZ, Heydari A, Halvaei I. A novel microfluidic system to separate sperm using spermatozoa inherent motion and inertial effect. J Biomech. 2022;142:111256. https://doi.org/10.1016/j.jbiomech.2022.111256.

22. Son J, Samuel R, Gale BK, Carrell DT, Hotaling JM. Separation of sperm cells from samples containing high concentrations of white blood cells using a spiral channel. Biomicrofluidics. 2017;11(5):054106. https://doi.org/10.1063/1.4994548.

23. Lara-Cerrillo S, Urda Munoz C, de la Casa Heras M, Camacho Fernandez-Pacheco S, de la Santa JG, Lacruz-Ruiz T, et al. Microfluidic sperm sorting improves ICSI outcomes in patients with increased values of double-strand breaks in sperm DNA. Rev Int Androl. 2022;21(1):100338. https://doi.org/10.1016/j.androl.2021.10.003.

24. Mohajeri M, Eskandari M, Ghazali ZS, Ghazali HS. Cell encapsulation in alginate-based microgels using droplet microfluidics; a review on gelation methods and applications. Biomed Phys Eng Express. 2022;8(2):022001. https://doi.org/10.1088/2057-1976/ac4e2d.

25. Badali E, Hosseini M, Varaa N, Mahmoodi N, Goodarzi A, Nooshabadi VT, et al. Production of uniform size cell-enclosing silk derivative vehicles through coaxial microfluidic device and horseradish crosslinking reaction. Eur Polym J. 2022;172:111237. https://doi.org/10.1016/j.eurpolymj.2022.111237.

26. Tung CK, Lin C, Harvey B, Fiore AG, Ardon F, Wu M, et al. Fluid viscoelasticity promotes collective swimming of sperm. Sci Rep. 2017;7(1):3152. https://doi.org/10.1038/s41598-017-03341-4.

27. Bahat A, Eisenbach M, Tur-Kaspa I. Periovulatory increase in temperature difference within the rabbit oviduct. Hum Reprod. 2005;20(8):2118–21. https://doi.org/10.1093/humrep/dei006.

28. Doostabadi MR, Mangoli E, Marvast LD, Dehghanpour F, Maleki B, Torkashvand H, et al. Microfluidic devices employing chemo- and thermotaxis for sperm selection can improve sperm parameters and function in patients with high DNA fragmentation. Andrologia. 2022;54(11):e14623. https://doi.org/10.1111/and.14623.

29. Penny JA, Lymbery RA, Evans JP, Sherman CDH, Conlan XA. The use of microfluidic devices in studies of differential sperm chemotaxis. Trends Biotechnol. 2022;40(10):1144–7. https://doi.org/10.1016/j.tibtech.2022.06.014.

30. Tung CK, Hu L, Fiore AG, Ardon F, Hickman DG, Gilbert RO, et al. Microgrooves and fluid flows provide preferential passageways for sperm over pathogen Tritrichomonas foetus. Proc Natl Acad Sci USA. 2015;112(17):5431–6. https://doi.org/10.1073/pnas.1500541112.

31. Huchzermeyer S, Wehrend A, Bostedt H. Histomorphology of the equine cervix. Anat Histol Embryol. 2005;34(1):38–41. https://doi.org/10.1111/j.1439-0264.2004.00565.x.

32. Miki K, Clapham DE. Rheotaxis guides mammalian sperm. Curr Biol. 2013;23(6):443–52. https://doi.org/10.1016/j.cub.2013.02.007.

33. Marzano G, Chiriaco MS, Primiceri E, Dell'Aquila ME, Ramalho-Santos J, Zara V, et al. Sperm selection in assisted reproduction: a review of established methods and cutting-edge possibilities. Biotechnol Adv. 2020;40:107498. https://doi.org/10.1016/j.biotechadv.2019.107498.

34. Vailati-Riboni M, Palombo V, Loor JJ. What are omics sciences? Periparturient diseases of dairy cows: a systems biology approach. 2017:1–7.

35. Khorani M, Bobe G, Matthews DG, Magana AA, Caruso M, Gray NE, et al. The impact of the hAPP695 SW transgene and associated amyloid-β accumulation on murine hippocampal biochemical pathways. J Alzheimers Dis. 2022;85:1601–19. https://doi.org/10.3233/JAD-215084.

36. Evans HC, Dinh TT, Hardcastle ML, Gilmore AA, Ugur MR, Hitit M, et al. Advancing semen evaluation using lipidomics. Front Vet Sci. 2021;8:601794. https://doi.org/10.3389/fvets.2021.601794.

37. Parker GHVII. The passage of sperms and of eggs through the oviducts in terrestrial vertebrates. Philos Trans Royal Soc Lond Ser B, Contain P Biol Character. 1931;219(462–467):381–419. https://doi.org/10.1098/rstb.1931.0008.

38. Lott G, Zur anatomie und physiologie des cervix uteri: Enke. 1872.

39. Smith DJ, Gaffney EA, Gadelha H, Kapur N, Kirkman-Brown JC. Bend propagation in the flagella of migrating human sperm, and its modulation by viscosity. Cell Motil Cytoskelet. 2009;66(4):220–36. https://doi.org/10.1002/cm.20345.

40. Seo DB, Agca Y, Feng ZC, Critser JK. Development of sorting, aligning, and orienting motile sperm using microfluidic device operated by hydrostatic pressure. Microfluid Nanofluid. 2007;3(5):561–70. https://doi.org/10.1007/s10404-006-0142-3.

41. Tung CK, Ardon F, Roy A, Koch DL, Suarez SS, Wu M. Emergence of upstream swimming via a hydrodynamic transition. Phys

Rev Lett. 2015;114(10):108102. https://doi.org/10.1103/PhysRevLett.114.108102.

42. Rappa K, Samargia J, Sher M, Pino JS, Rodriguez HF, Asghar W. Quantitative analysis of sperm rheotaxis using a microfluidic device. Microfluid Nanofluid. 2018;22(9):100. https://doi.org/10.1007/s10404-018-2117-6.

43. Heydari A, Zabetian Targhi M, Halvaei I, Nosrati R. A novel microfluidic device with parallel channels for sperm separation using spermatozoa intrinsic behaviors. Sci Rep. 2023;13(1):1185. https://doi.org/10.1038/s41598-023-28315-7.

44. Wu JK, Chen PC, Lin YN, Wang CW, Pan LC, Tseng FG. High-throughput flowing upstream sperm sorting in a retarding flow field for human semen analysis. Analyst. 2017;142(6):938–44. https://doi.org/10.1039/c6an02420c.

45. Zaferani M, Cheong SH, Abbaspourrad A. Rheotaxis-based separation of sperm with progressive motility using a microfluidic corral system. Proc Natl Acad Sci USA. 2018;115(33):8272–7. https://doi.org/10.1073/pnas.1800819115.

46. Zaferani M, Palermo GD, Abbaspourrad A. Strictures of a microchannel impose fierce competition to select for highly motile sperm. Sci Adv. 2019;5(2):eaav2111. https://doi.org/10.1126/sciadv.aav2111.

47. El-Sherry TM, Elsayed M, Abdelhafez HK, Abdelgawad M. Characterization of rheotaxis of bull sperm using microfluidics. Integr Biol (Camb). 2014;6(12):1111–21. https://doi.org/10.1039/c4ib00196f.

48. El-Sherry TM, Abdel-Ghani MA, Abou-Khalil NS, Elsayed M, Abdelgawad M. Effect of pH on rheotaxis of bull sperm using microfluidics. Reprod Domest Anim. 2017;52(5):781–90. https://doi.org/10.1111/rda.12979.

49. Romero-Aguirregomezcorta J, Sugrue E, Martinez-Fresneda L, Newport D, Fair S. Hyperactivated stallion spermatozoa fail to exhibit a rheotaxis-like behaviour, unlike other species. Sci Rep. 2018;8(1):16897. https://doi.org/10.1038/s41598-018-34973-9.

50. Zaferani M, Javi F, Mokhtare A, Abbaspourrad A. Effect of flagellar beating pattern on sperm rheotaxis and boundary-dependent navigation. BioRxiv. 2020. https://doi.org/10.1101/2020.01.20.913145.

51. De Martin H, Cocuzza MS, Tiseo BC, Wood GJA, Miranda EP, Monteleone PAA, et al. Positive rheotaxis extended drop: a one-step procedure to select and recover sperm with mature chromatin for intracytoplasmic sperm injection. J Assist Reprod Genet. 2017;34(12):1699–708. https://doi.org/10.1007/s10815-017-1024-1.

52. Sarbandi IR, Lesani A, Moghimi Zand M, Nosrati R. Rheotaxis-based sperm separation using a biomimicry microfluidic device. Sci Rep. 2021;11(1):18327. https://doi.org/10.1038/s41598-021-97602-y.

53. Nagata MPB, Endo K, Ogata K, Yamanaka K, Egashira J, Katafuchi N, et al. Live births from artificial insemination of microfluidic-sorted bovine spermatozoa characterized by trajectories correlated with fertility. Proc Natl Acad Sci USA. 2018;115(14):E3087–96. https://doi.org/10.1073/pnas.1717974115.

54. Sharma S, Kabir MA, Asghar W. Selection of healthy sperm based on positive rheotaxis using a microfluidic device. Analyst. 2022;147(8):1589–97. https://doi.org/10.1039/d1an02311j.

55. Eamer L, Vollmer M, Nosrati R, San Gabriel MC, Zeidan K, Zini A, et al. Turning the corner in fertility: high DNA integrity of boundary-following sperm. Lab Chip. 2016;16(13):2418–22. https://doi.org/10.1039/c6lc00490c.

56. Denissenko P, Kantsler V, Smith DJ, Kirkman-Brown J. Human spermatozoa migration in microchannels reveals boundary-following navigation. Proc Natl Acad Sci USA. 2012;109(21):8007–10. https://doi.org/10.1073/pnas.1202934109.

57. Nosrati R, Graham PJ, Liu Q, Sinton D. Predominance of sperm motion in corners. Sci Rep. 2016;6(1):26669. https://doi.org/10.1038/srep26669.

58. Nosrati R, Vollmer M, Eamer L, San Gabriel MC, Zeidan K, Zini A, et al. Rapid selection of sperm with high DNA integrity. Lab Chip. 2014;14(6):1142–50. https://doi.org/10.1039/c3lc51254a.

59. Organization WH. WHO laboratory manual for the examination and processing of human semen. 2010.

60. Brinsko SP, Blanchard TL, Varner DD, Schumacher J, Love CC. Manual of equine reproduction-E-book. Amsterdam: Elsevier Health Sciences; 2010.

61. Bartoov B, Berkovitz A, Eltes F, Kogosowski A, Menezo Y, Barak Y. Real-time fine morphology of motile human sperm cells is associated with IVF-ICSI outcome. J Androl. 2002;23(1):1–8. https://doi.org/10.1002/j.1939-4640.2002.tb02595.x.

62. De Vos A, Van de Velde H, Bocken G, Eylenbosch G, Franceus N, Meersdom G, et al. Does intracytoplasmic morphologically selected sperm injection improve embryo development? A randomized sibling-oocyte study. Human Reprod. 2013;28(3):617–26. https://doi.org/10.1093/humrep/des435.

63. Belva F, Bonduelle M, Roelants M, Michielsen D, Van Steirteghem A, Verheyen G, et al. Semen quality of young adult ICSI offspring: the first results. Hum Reprod. 2016;31(12):2811–20.

64. Huang HY, Wu TL, Huang HR, Li CJ, Fu HT, Soong YK, et al. Isolation of motile spermatozoa with a microfluidic chip having a surface-modified microchannel. Jala-J Lab Autom. 2014;19(1):91–9. https://doi.org/10.1177/2211068213486650.

65. Cho BS, Schuster TG, Zhu X, Chang D, Smith GD, Takayama S. Passively driven integrated microfluidic system for separation of motile sperm. Anal Chem. 2003;75(7):1671–5. https://doi.org/10.1021/ac020579e.

66. Zhang B, Yin TL, Yang J. A novel microfluidic device for selecting human sperm to increase the proportion of morphologically normal, motile sperm with uncompromised DNA integrity. Anal Methods. 2015;7(14):5981–8. https://doi.org/10.1039/c5ay00905g.

67. Asghar W, Velasco V, Kingsley JL, Shoukat MS, Shafiee H, Anchan RM, et al. Selection of functional human sperm with higher DNA integrity and fewer reactive oxygen species. Adv Healthc Mater. 2014;3(10):1671–9. https://doi.org/10.1002/adhm.201400058.